Physical properties of Class I methanol masers

Silvia Leurini[1] and Karl M. Menten[2]

[1]INAF - Osservatorio Astronomico di Cagliari
Via della Scienza 5, 09047, Selargius (CA), Italy
email: `sleurini@oa-cagliari.inaf.it`

[2]Max-Planck-Institut für Radioastronomie
Auf Dem Hügel 69, 53121, Bonn, Germany
email: `kmenten@mpifr.de`

Abstract. As first realised in the late 1980s, methanol masers come in two varieties, termed Class I and Class II. While Class II masers had observationally been extensively studied in the past, until recently relatively little attention was paid to Class I methanol masers due to their low luminosities compared to other maser transitions. In this review, we will focus on the recent progress in our understanding of Class I methanol masers both from an observational and from a theoretical point of view.

Keywords. masers, ISM: molecules

1. Introduction – the two classes of methanol masers

Methanol masers are common phenomena in regions of massive star formation. Early studies empirically revealed two different classes based on observational properties (Wilson *et al.* 1985; Batrla *et al.* 1987). These were termed Class I and Class II (Menten 1991a). Soon after, it was also recognised (Menten 1991b) that different pumping mechanisms produce inversion in Class I methanol masers (CIMMs), first detected in a series of lines near 25 GHz (Barrett *et al.* 1971) and, later, at 36 GHz and 44 GHz (Morimoto *et al.* 1985) on the one hand and in Class II methanol masers (CIIMMs) on the other. The most common CIIMM transition is by far the 6.7 GHz line, followed by the 12.18 GHz line (Menten 1991a; Batrla *et al.* 1987).

CIIMMs are found in the closest environment of massive young stellar objects (MYSOs) and are pumped by the intense mid-infrared radiation from these objects' dense dust shells. Their presence is actually a sufficient, if not a necessary, signpost for a MYSO (Urquhart *et al.* 2015). Early calculations (e.g., Cragg *et al.* 1992) showed that inversion population in CIIMMs happens when the brightness temperature of the external radiation is greater than the kinetic temperature of the gas. Sobolev & Deguchi (1994) and Sobolev *et al.* (1997) first suggested that CIIMMs are excited through the pumping of molecules from the torsional ground state to rotational energy levels within the torsionally excited $v_t = 1, 2$ states as consequence of absorption of mid-infrared photons followed by cascade back to the ground state. Later, Cragg *et al.* (2005) examined the effects of including higher energy levels, and found that this effect is significant only at dust temperatures above 300 K. One should notice, however, that up to now models of CIIMMs have only made use of limited sets of collisional rates and that the results of new calculations of Rabli & Flower (2010, 2011) have not been implemented yet. It is of paramount importance to revise models of CIIMMs in light of these new calculations and investigate in details the exact pumping cycle of CIIMMs.

CIMMs are, on the other hand, collisionally pumped and their occurrence can be explained from the basic properties of the CH_3OH molecule (Lees 1973). First statistical equilibrium studies on CIMMs made use of collisional rates based on experimental results by Lees & Oka (1969) and Lees & Haque (1974). These rates show a propensity for $\Delta k = 0$ collisions and a dependence upon ΔJ as $1/\Delta J$. The propensity for $\Delta k = 0$ over $\Delta k = 0, 1$ collisions causes molecules to preferentially de-excite down a k stack, causing overpopulation in the lower levels in the $k = -1$ stack for CH_3OH-E, leading to maser action in the $J_{-1} \rightarrow (J-1)_0$-$E$ series and to enhanced absorption ($\equiv$ anti-inversion) in the $2_0 \rightarrow 3_{-1}$-E line (Walmsley *et al.* 1988). An analogous situation holds for the $K = 0$ ladder of CH_3OH-A, leading to the $J_0 \rightarrow (J-1)_1$-A^+ masers and also to the anti-inversion of the $5_1 \rightarrow 6_0$-A^+ transition†. However, while previously used collisional rates can reproduce the anti-inversion at $12.18\,\mathrm{GHz}$ and $6.7\,\mathrm{GHz}$ and inversion for many CIMM lines, they do not account for the $J_2 \rightarrow J_1$-E series of masers at $25\,\mathrm{GHz}$. For this reason, ad hoc selection rules were adopted to reproduce inversion population in these transitions (e.g., Johnston *et al.* 1992 and Cragg *et al.* 1992). Recent models (McEwen *et al.* 2014; Nesterenok 2016) have confirmed that CIMMs mase in different density ranges.

In this contribution, we review the observational and theoretical properties of CIMMs in view of the increasing interests that these masers gained over the last decades not only in the star formation community but also in other fields of astronomy.

2. Overview of observational properties of CIMMs

CIMMs are associated with astrophysical shocks. They are often observed in the swept-up interaction region of outflows with ambient material predominantly from MYSOs (Plambeck & Menten 1990), but also from low-mass YSOs, (e.g. Kalenskii *et al.* 2010; Rodríguez-Garza *et al.* 2017). They have also been detected in the interaction regions of supernova remnants with the molecular clouds (e.g., Szczepanski *et al.* 1989; Haschick *et al.* 1990; Pihlstrom *et al.* 2011), in cloud-cloud collisions (e.g. Sobolev 1992), and in layers where expanding HII regions interact with the ambient molecular environment (Voronkov *et al.* 2010). Finally, over the last years detections of CIMMs were reported also in external galaxies (e.g., in NGC 253 and NGC 4945 by Ellingsen *et al.* 2014 and 2017, and McCarthy *et al.* 2017) with emission reported to be up to 10^5 times more luminous than the corresponding Galactic CIMMs.

In the last decade, CIMMs were routinely used as signposts of star formation activity, especially in very early phases of massive star formation for which it is difficult to detect outflow activity in mid-infrared observations due to high extinction (e.g., Cyganowski *et al.* 2009, Yanagida *et al.* 2014, Towner *et al.* 2017). The recent detection of circular polarization in CIMMs lines shows these masers' potential for probes of magnetic fields in interstellar shocks (Sarma & Momjian 2009, 2011). Finally, their association with supernova remnants make CIMMs interesting tracer of density which may be useful for modeling of cosmic ray particle acceleration (Frail 2011).

CIMMs in regions of massive star formation have typical luminosities of $10^{-5}-10^{-6}\,\mathrm{L_\odot}$, spot sizes are of the order of tens of AU based on VLA observations of the $6_2 \rightarrow 6_1$-E line at $25.018\,\mathrm{GHz}$ (Johnston *et al.* 1997) and the recent first VLBI detection of the $7_0 \rightarrow 6_1$-A^+ maser at $44\,\mathrm{GHz}$ (Matsumoto *et al.* 2014). In star-forming regions, the $44\,\mathrm{GHz}$ CIMM is usually stronger than the other transitions: Voronkov *et al.* (2014) found

---

† We note that a strong IR field causes the $5_1 \rightarrow 6_0$-A^+ and the $2_0 \rightarrow 3_{-1}$-E line to become the most prominent Class II *maser* transitions.
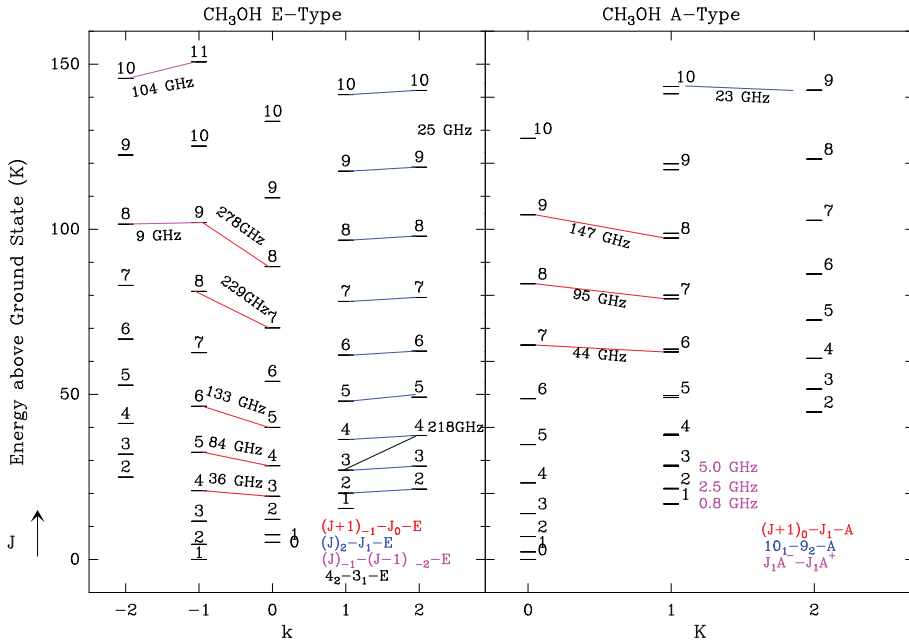
Figure 1. Partial rotational level diagram of *E*-type (right) and *A*-type (left) methanol (adapted from Leurini *et al.* 2016). Different colours (see the on-line version of the Figure) are used for different families of transitions: red indicates the $(J+1)_1 \to J_0$-*E* (left) and the $(J+1)_0 \to J_1$-*A* series (right), blue the $J_2 \to J_1$-*E* series (left) and the $10_1 \to 9_2$-*A* line (right), magenta the $(J-1) \to (J-1)_{-2}$-*E* series (left) and the $J_1 A^- \to J_1 A^+$ transitions (right), black the $4_2 \to 3_1$-*E* maser (left).

that the 36 GHz line ($4_{-1} \to 3_0$-*E*) is stronger than the 44 GHz maser only in 40 out of 292 maser spots in a recent survey of massive star-forming regions in both transitions. On the contrary, toward supernova remnants, the 36 GHz line is often stronger than the 44 GHz transition and in some cases the latter is completely absent (e.g, Pihlström *et al.* 2014). Recently, Ellingsen *et al.* (2017) suggested that extragalactic CIMMs (at least in NGC 253) have similar properties than those in supernova-molecular cloud interactions.

3. Statistical equilibrium calculations

In the following, we will review the recent results from Leurini *et al.* (2016) and complement their analysis with the discussion of other rarer CIMMs. In particular, we will report on the properties of the $9_{-1} \to 8_{-2}$-*E* 9.9 GHz, $10_1 \to 9_2$-A^- 23.4 GHz, and $11_{-1} \to 10_{-2}$-*E* 104 GHz lines; see Voronkov *et al.* (2012) for a detailed discussion of their observational properties. We also discuss predictions for the low-frequency $J_1 A^- \to J_1 A^+$ doublet transitions, the lowest of which ($J = 1$ at 834 MHz) is the first CH_3OH line discovered in the interstellar medium (Ball *et al.* 1970). Our main focus are CIMMs in regions of massive star formation. All lines discussed in this paper are shown in Fig. 1. For models of CIMMs in supernova remnants, we refer the reader to McEwen *et al.* (2014).

Following the formalism developed by Elitzur *et al.* (1989) and Hollenbach *et al.* (2013) for H_2O masers, we use the pump rate coefficient, q, the maser loss rate, Γ, and the inversion efficiency of the pumping scheme, η (see Eqs. 6–8 in Leurini *et al.* 2016) to define the photon production rate $\Phi_m = \frac{g_u g_l}{g_u + g_l} \times 2n^2 X(CH_3OH)\eta q$ to characterise the maser emission (g_u and g_l are the statistical weights for the upper and lower levels of

a given maser system). Indeed, the photon production rate at line centre of a saturated maser transition is directly linked to its observed flux through the geometry of the maser. Therefore, under the assumption that different maser lines are emitted by the same volume of gas and that they are saturated, the ratio of the photon production rates of two lines is directly proportional to the ratio between the observed fluxes of those lines.

3.1. The low-frequency $J_1\,A^- \to J_1\,A^+$ transitions

Low-frequency transitions in the $J_1\,A^- \to J_1\,A^+$ series were detected in emission at 834 MHz and 5005 MHz towards bright centimeter continuum sources in the Central Molecular Zone (CMZ) surrounding the Galactic center (e.g., Ball *et al.* 1970, Robinson *et al.* 1974, Mezger & Smith 1976). Given that their flux densities are only a small fraction of that of continuum background radiation, these lines do clearly not show high gain maser action. High angular and velocity resolution observations are not available to directly confirm their maser nature. However, not only are they in emission against the CMZ's very strong radio continuum emission, they are also associated with absorption in the 12.18 GHz line toward at least two lines of sight (Peng & Whiteoak 1992). As explained in Section 1, *absorption* in this line, which is a cardinal CIIMM transition, is characteristic of CIMMs. This strongly suggests that the $J_1\,A^- \to J_1\,A^+$ lines are weak CIMMs. Indeed, previous calculations from Cragg *et al.* (1992) confirmed that these lines are inverted over a broad range of physical parameters. Their inversion under the special physical (and chemical) conditions of the CMZ follows a pattern observed for low radio frequency lines of several other molecules; see Menten (2004) for a discussion.

Our modelling predicts inversion in the low-frequency $J_1\,A^- \to J_1\,A^+$ transitions (and in all other lines for which maser emission is observed, see Fig. 1). The $J_1\,A^- \to J_1\,A^+$ series has low opacities ($|\tau| < 0.4$) and is inverted over a broad range of densities and temperatures. The brightest of the series is the $1_1\,A^- \to 1_1\,A^+$ line at 834 MHz.

3.2. Modelling results

We investigated the behaviour of the photon production rate Φ_m as function of the physics of the gas for the most common $(J+1)_{-1} - J_0$-E, $(J+1)_0 - J_1$-A and $J_2 - J_1$-E CIMMs and for the rarer 9.9 GHz, 23.4 GHz and 104 GHz lines. The computations show that for all these CIMMs, Φ_m grows with the emission measure ξ, the ratio of the product of the molecular hydrogen and methanol number densities over the velocity (see Eqs. 3 and 5 in Leurini *et al.* 2016). Therefore, bright CIMMs trace high methanol emission measures. These values are reached at high densities, high temperatures, and high methanol column densities. Moreover, all bright CIMMs (the $(J+1)_{-1} - J_0$-E, $(J+1)_0 - J_1$-A and $J_2 - J_1$-E series) quench at a constant specific column density of some $10^{17}\,\mathrm{cm}^{-2}\,\mathrm{km}^{-1}\,\mathrm{s}$ independently of volume density as long as it is in the range $10^5 - 10^7\,\mathrm{cm}^{-3}$, suggesting that there is a critical methanol column density at which quenching occurs. The rare CIMM lines at 9.9 GHz, 104 GHz and 23.4 GHz seem to trace more extreme conditions than the more common CIMM lines in terms of density, column density and temperature as already suggested by previous models (see Sobolev *et al.* 2005).

Leurini *et al.* (2016) showed that CIMMs can be divided in at least three families, depending on their behaviour as function of photon production rate: the $(J+1)_{-1} - J_0$-E type series, the $(J+1)_0 - J_1$-A type and the $J_2 - J_1$-E series at 25 GHz. They differ in the slope of the Φ_m dependence on ξ and on density. This is well illustrated in Fig. 2 (adapted from Figs. 10 and 12 of Leurini *et al.* 2016) where ratios between photon production rates of different masers are plotted as function of the emission measure: while ratios between Φ_m of lines in within the same family are relatively flat (left panel),
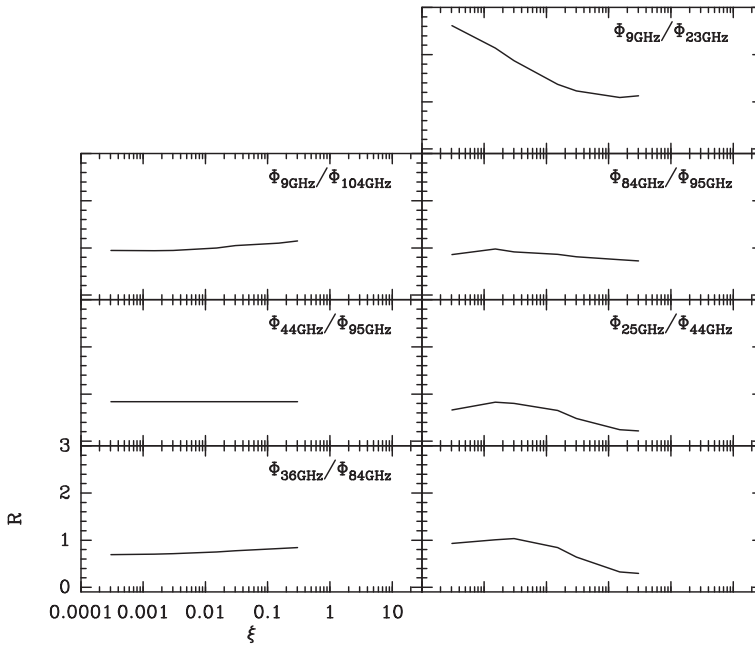
Figure 2. Modelled ratios between photon production rates of several CIMMs for $T = 200\,K$ and a volume density $n = 10^7\,\mathrm{cm}^{-3}$. In the left panel, we show ratios among transitions within same families, while in the right panel we plot ratios among CIMMs from different families.

ratios among different families have a strong dependence on ξ (right panel). The ratio of the $\Phi_{9.9\mathrm{GHz}}$ to $\Phi_{23.4\mathrm{GHz}}$ shows the strongest dependence on the physics of the gas. In addition, the $J_2 - J_1$-E lines have a much flatter ξ dependence than the other lines at high densities (Fig. 12 in Leurini *et al.* 2016).

4. Conclusions

CIMMs are powerful tools to investigate the physics of astrophysical shocks. Our calculations show that

• The production rates of all known CIMMs increase with ξ till thermalisation is reached. Therefore, bright CIMMs trace high methanol emission measure reached at high densities ($n(\mathrm{H}_2) \sim 10^7 - 10^8\,\mathrm{cm}^{-3}$), high temperatures ($> 100\,\mathrm{K}$) and high methanol column densities;

• CIMMs can reasonably be separated into different families depending on the behaviour of their photon production rate as function of ξ;

• The 25 GHz lines and the rare lines at 9.9 GHz, 23.4 GHz and 104 GHz trace higher densities and temperatures than the other lines.

This contribution, as this whole conference, is dedicated to the memory of Malcolm Walmsley.

References

Ball, J. A., Gottlieb, C. A., Lilley, A. E., & Radford, H. E. 1970, *Ap. Lett.*, 162, L203
Barrett, A. H., Schwartz, P. R., & Waters, J. W. 1971, *ApJ*, 168, L101
Batrla, W., Matthews, H. E., Menten, K. M., & Walmsley, C. M. 1987, *Nature*, 326, 49
Cragg, D. M., Johns, K. P., Godfrey, P. D., & Brown, R. D. 1992, *MNRAS*, 259, 203

Cragg, D. M., Sobolev, A. M., & Godfrey, P. D. 2005, *MNRAS*, 360, 533

Cyganowski, C. J., Brogan, C. L., Hunter, T. R., & Churchwell, E. 2009, *ApJ*, 702, 1615

Ellingsen, S. P., Chen, X., Qiao, H.-H., *et al.* 2014, *ApJ*, 790, L28

Ellingsen, S. P., Chen, X., Breen, S. L., & Qiao, H.-H. 2017, *MNRAS*, 472, 604

Elitzur, M., Hollenbach, D. J., & McKee, C. F. 1989, *ApJ*, 346, 983

Frail, D. A. 2011, *Mem. Soc. Astr. Italiana*, 82, 703

Haschick, A. D., Menten, K. M., & Baan, W. A. 1990, *ApJ*, 354, 556

Hollenbach, D., Elitzur, M., & McKee, C. F. 2013, *ApJ*, 773, 70

Johnston, K. J., Gaume, R., Stolovy, S., *et al.* 1992, *ApJ*, 385, 232

Johnston, K. J., Gaume, R. A., Wilson, T. L., Nguyen, H. A., & Nedoluha, G. E. 1997, *ApJ*, 490, 758

Kalenskii, S. V., Johansson, L. E. B., Bergman, P., *et al.* 2010, *MNRAS*, 405, 613

Lees, R. M. 1973, *ApJ*, 184, 763

Lees, R. M. & Oka, T. 1969, *J. Chem. Phys*, 51, 3027

Lees, R. M. & Haque, S. 1974, *Can. J. Phys.*, 52, 2250

Leurini, S., Menten, K. M., & Walmsley, C. M. 2016, *A&A*, 592, A31

McCarthy, T. P., Ellingsen, S. P., Chen, X., *et al.* 2017, *ApJ*, 846, 156

Matsumoto, N., Hirota, T., Sugiyama, K., *et al.* 2014, *Ap. Lett.*, 789, L1

McEwen, B. C., Pihlström, Y. M., & Sjouwerman, L. O. 2014, *ApJ*, 793, 133

Menten, K. M. 1991a, *ApJ*, 380, L75

Menten, K. 1991b, Atoms, Ions and Molecules: New Results in Spectral Line Astrophysics, 16, 119

Menten, K. M. 2004, in *The Dense Interstellar Medium in Galaxies*, 91, 69

Mezger, P. G. & Smith, L. F. 1976, *A&A*, 47, 143

Morimoto, M., Kanzawa, T., & Ohishi, M. 1985, *ApJ*, 288, L11

Nesterenok, A. V. 2016, *MNRAS*, 455, 3978

Peng, R. S. & Whiteoak, J. B. 1992, *MNRAS*, 254, 301

Pihlström, Y. M., Sjouwerman, L. O., & Fish, V. L. 2011, *Ap. Lett.*, 739, L21

Pihlström, Y. M., Sjouwerman, L. O., Frail, D. A., *et al.* 2014, *AJ*, 147, 73

Plambeck, R. L. & Menten, K. M. 1990, *ApJ*, 364, 555

Rabli, D. & Flower, D. R. 2010, *MNRAS*, 406, 95

Rabli, D. & Flower, D. R. 2011, *MNRAS*, 411, 2093

Robinson, B. J., Brooks, J. W., Godfrey, P. D., & Brown, R. D. 1974, *Australian Journal of Physics*, 27, 865

Rodríguez-Garza, C. B., Kurtz, S. E., Gómez-Ruiz, A. I., *et al.* 2017, arXiv:1709.09773

Sarma, A. P. & Momjian, E. 2009, *Ap. Lett.*, 705, L176

Sarma, A. P. & Momjian, E. 2011, *Ap. Lett.*, 730, L5

Sobolev, A. M. 1992, *Soviet Astron.*, 36, 590

Sobolev, A. M. & Deguchi, S. 1994, *A&A*, 291, 569

Sobolev, A. M., Cragg, D. M., & Godfrey, P. D. 1997, *A&A*, 324, 211

Sobolev, A. M., Ostrovskii, A. B., Kirsanova, M. S., *et al.* 2005, Massive Star Birth: A Crossroads of Astrophysics, 227, 174

Szczepanski, J. C., Ho, P. T. P., Haschick, A. D., & Baan, W. A. 1989, The Center of the Galaxy, 136, 383

Towner, A. P. M., Brogan, C. L., Hunter, T. R., *et al.* 2017, *ApJS*, 230, 22

Urquhart, J. S., Moore, T. J. T., Menten, K. M., *et al.* 2015, *MNRAS*, 446, 3461

Voronkov, M. A., Caswell, J. L., Ellingsen, S. P., & Sobolev, A. M. 2010, *MNRAS*, 405, 2471

Voronkov, M. A., Caswell, J. L., Ellingsen, S. P., *et al.* 2012, Cosmic Masers - from OH to H0, 287, 433

Voronkov, M. A., Caswell, J. L., Ellingsen, S. P., Green, J. A., & Breen, S. L. 2014, *MNRAS*, 439, 2584

Yanagida, T., Sakai, T., Hirota, T., *et al.* 2014, *Ap. Lett.*, 794, L10

Walmsley, C. M., Batrla, W., Matthews, H. E., & Menten, K. M. 1988, *A&A*, 197, 271

Wilson, T. L., Walmsley, C. M., Menten, K. M., & Hermsen, W. 1985, *A&A* 147, L19